ORIGINAL ARTICLE

# A Statistical Evaluation Model for the Time-dependent Strength of Cement-admixed Marine Clay

**Yong Liu**[1], **Huawen Xiao**[2*], **Hui Liu**[3], **Guicai Shi**[4]

[1] State Key Laboratory of Water Resources and Hydropower Engineering Science, Wuhan University, Wuhan, P.R.China

[2*] Golder Associates, 329983, Singapore (Corresponding author)

[3] School of Civil Engineering and Architecture, Hainan University, Haikou 570228,China

[4] School of Civil Engineering and Architecture, Changzhou Institute of Technology, Changzhou 213022, China

***Abstract:*** Deep Cement Mixing (DCM) is widely used in urban infrastructure construction such as deep excavation and tunnelling. The variability of the properties of natural soils, combined with uncertainty and inaccuracy of construction operation of deep soil mixing, leads to non-uniformity of the binder distribution in the deep cement-mixed soil, therefore, the often highly variable strength. This study investigates the point level of the unconfined compressive strength of cement-stabilized soils. A statistical approach to evaluate the heterogeneous strength of cement-admixed marine clay is proposed. The unconfined compressive strength of cemented clay is regarded as a random variable with the probability density distribution being assumed as the lognormal distribution. Particularly, the curing time effect is considered in the approach. A simple time-dependent probability density distribution is proposed, with only the mean value changing to account for the curing time effect.

***Keywords:*** Cement-treated marine clay; Unconfined compressive strength; Curing time effect statistical analysis; Random variable

## 1. Introduction

It is important to maximise the use of underground space in metropolises (e.g. Shanghai, Singapore) for further development of the society. For instance, around 25% of the land area in Singapore is underlain by soft marine clay with the undrained shear strength ranging from approximately 15kPa to 35kPa[1]. Due to its high-water content, high compressibility and low shear strength, dealing with marine clay poses many difficulties for Civil Engineers. Underground space construction such as deep excavation and tunnelling for MRT has been a challenging issue in these soft soil areas, especially where there are many buildings around the construction. It is because that any form of disturbance to the soil might induce ground movement, which may lead to cracks or even collapse of the nearby infrastructures. In this situation, ground improvement for soft soils is necessary before underground construction to prevent collapse as well as minimise ground movements and disturbance to nearby structures.

Deep Cement Mixing (DCM) is a commonly used technology in ground improvement by introducing cementitious binder to the soft soils. DCM typically takes place by mechanical dry mixing, wet mixing or, grouting[2—4]. Dry mixing is available in the sites where water content is high. Wet mixing is recommended for sites with deep water table locations or dry and arid environments. Grouting has been adopted for ground strengthening or excavation support[3,5], . To control the quality and the cost of the underground construction as well as reduce the impact to the environment in duced by the construction, stiffness and strength are two most critical properties for the cement improved soil. The stiffness has been studied by many researches[6—12]. The strength of cemented clay in DCM has also been extensively

Copyright © 2018 Yong Liu *et al*.
doi: 10.18686/utc.v4i2.34
This is an open-access article distributed under the terms of the Creative Commons Attribution Unported License (http://creativecommons.org/licenses/by-nc/4.0/), which permits unrestricted use, distribution, and reproduction in any medium, provided the original work is properly cited.

investigated[9,13—16]. The unconfined compressive strength is usually treated as invariable for given curing days. However, for the deep-mixed soil mass, highly variable strength is often observed due to the non-uniform binder distribution in the columns. Both in-situ cases and physical model tests reported that the concentration of binder and spot strength of the DCM columns is highly variable[17—24]. Some key factors will lead to the spatial variability, e.g., the variability of the properties of natural soils, the uncertainty and inaccuracy of construction operation of DCM. Therefore, the range of strength variation of cemented soil is usually much larger than that of natural cohesive soil. In design, this heterogeneity of the stabilized soil poses challenges for the Engineers. This is because the strength of stabilized soil as a mass cannot be thoroughly evaluated from the unconfined compressive strength of cored specimens.

Some statistical approaches are studied to deal with this problem[17,25-27]. For instance, Liu *et al*.'s (2008) work[26] was extended from the following strength function of cement-admixed marine clay

$$q_{\mathrm{u}} = q_0[e^{m(s/c)}/(w/c)^n] \tag{1}$$

where $q_u$ is the unconfined compressive strength of cement-admixed marine clay; $q_0$, m and n are experimentally fitted values; $w$ = mass ratio of water in cemented admixed soft soil; $c$ = mass ratio of cement; $s$ = mass ratio of soil. **Figure 1** shows the phase relationship among w, c and s within a cement-admixed soil sample. Eq. 1 was proposed by[15]. However, the curing time effect of cement-admixed marine clay has not been considered by Eq. 1. In this regard, [16] and[9] proposed the following evaluation model for Ordinary Portland Cement treated marine clay:

$$q_{\mathrm{u}} = q_\infty \left\{ 1 - \frac{1}{1+(\frac{at}{q_\infty})^r} \right\} \left\{ \frac{\exp\left(m\left(s/c\right)\right)}{\left(\frac{w}{c}\right)^n} \right\} \tag{2}$$

where $q_\infty$ is the long-term value for $q_0$; α is the initial rate of increase in $q_0$ with time; r is a fitted index. Based on Xiao *et al*.'s (2014) work[16], the basic parameters in Eqs. 1 and 2 for cement-admixed marine clay are listed in **Table 1**.

Based on Eq. 2, this study examined the statistical behaviour of the cement-admixed marine clay. The curing time effect is taken into consideration. Finally, a statistical evaluation model for the time-dependent strength of cement-admixed marine clay is proposed.

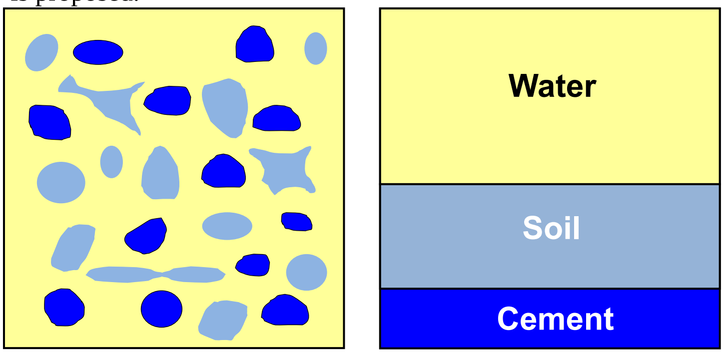


**Figure 1.** Illustration of soil, water and cement within a cement-admixed soil sample (left) randomly distributed within a sample, (right) schematic illustration of the phase relationship

# 2. Statistical analysis of strength function

For a given point of a cement-admixed marine column, the unconfined compressive strength $q_u$ can be predicted by using Eq. 2. To make it amenable to statistical analysis, Eq. 2 can be rewritten as

$$\ln q_{\mathrm{u}} = \ln q_\infty - \ln\left\{\left(\frac{q_\infty}{at}\right)^r + 1\right\} + m(\frac{s}{c}) - n\ln(w) + n\ln(c) \tag{3}$$

It can be found that the there are several terms on the right-hand side of Eq. 3. At a given curing time, there are only three state variables, that is, the mass ratios of cement, water and soil (i.e. c, s and w). Based on large volume of centrifuge model test data (see [28]), the mass ratio of cement in an admixture generally follows the normal distribution. However, no information on the distribution of s and w is found. In this regard, as shown in **Figure 1**, the distribution of the three components within a sample should be symmetric. Without other information, it is not unreasonable to assume both s and w also follow the normal distribution. Even so, the analytical probability density distribution (PDF) of $q_u$ in Eq. 3 is unlikely to be achieved. Nevertheless, the term $\ln(q_u)$ may be assumed to follow the normal distribution according to the central limit theorem. This theorem states that, when independent random variables are added, their properly normalized sum in most situations tends toward a normal distribution even if the original variables themselves are not normally distributed. As such, $q_u$ follows the lognormal distribution for a given curing time, with the following PDF:

$$f(q_u) = \frac{1}{\sqrt{2\pi}\sigma_{\ln} q_u} \exp\left\{ -\frac{1}{2} \left(\frac{\ln q_u - \mu_{\ln}}{\sigma_{\ln}}\right)^2 \right\}, 0 \le q_u < +\infty \tag{4}$$

where the parameters $\mu_{\ln}$ and $\sigma_{\ln}$, which are essentially the mean and standard deviation of $\ln(q_u)$, can be obtained from the relations:

$$\mu_{\ln} = \ln(\mu_{qu}) - \frac{1}{2}\sigma_{qu}^2 \tag{5}$$

$$\sigma_{\ln} = \sqrt{\ln(1 + \sigma_{qu}^2 / \mu_{qu}^2)} \tag{6}$$

in which $\mu_q$ and $\sigma_{qu}$ represent the mean value (i.e. expectation) and standard deviation of $q_u$, respectively. Therefore, two parameters of fitted lognormal distribution may be determined by the values of $\mu_q$ and $\sigma_{qu}$. To check the validation of the normal assumption of the term $\ln(q_u)$, the Monte-Carlo simulation technique with $10^4$ realizations is used: according to the normal distribution, $10^4$ random seeds of w and c are generated (see Figures 2a and 2b). One can obtain s = 1 – c – w based on the phase relationship shown in **Figure 1**, and the histogram of s is shown in **Figure 2c**. Then, substituting each set of random seed for s, w and c into Eq. 3 so that a sample of $10^4$ $\ln(q_u)$ values can be obtained, whereby the Kolmogorov–Smirnov test can be conducted for the normal assumption of the term $\ln(q_u)$. **Figure 3** shows the resultant histograms of $q_u$ and $\ln(q_u)$ from the $10^4$ Monte-Carlo simulations. It can be found that the shape of histogram of $q_u$ is lognormal and the histogram of $\ln(q_u)$ is a bell shape. Kolmogorov–Smirnov test on the histogram shown in **Figure 3b** indicate that the data cannot be rejected for the normal distribution assumption under a significant level of 0.05.

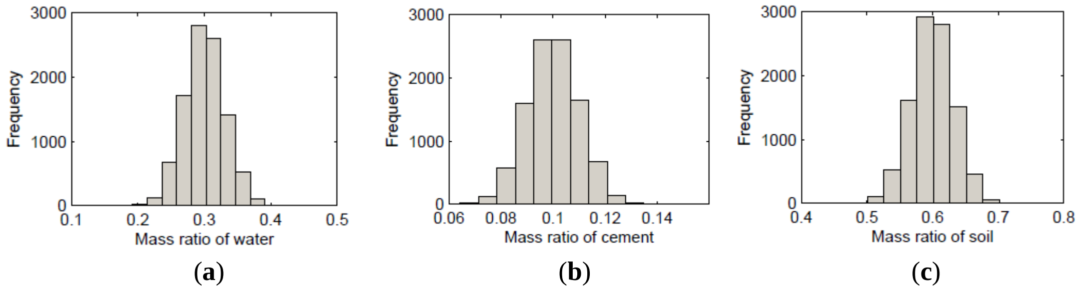


**Figure 2.** Histograms of (**a**) mass ratio of water, (**b**) mass ratio of cement and (**c**) mass ratio of soil in Monte-Carlo simulations

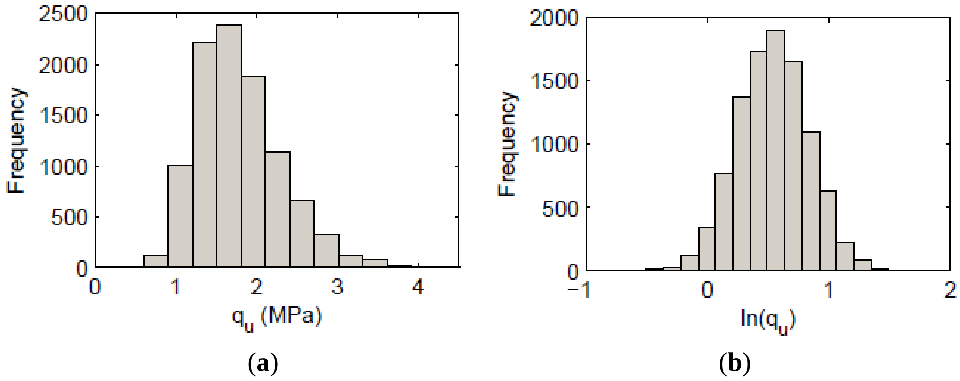


**Figure 3.** Histograms of resultant strength calculated with Eq. 3 from the data shown in **Figure 2**. (**a**) Unconfined compressive strength $q_u$, (**b**) $\ln(q_u)$

| Parameters | q∞ (MPa) | T (day) | α (MPa/day) | r | m | n | s | c | w |
|---|---|---|---|---|---|---|---|---|---|
| **Mean** | 40 | 28 | 1.3 | 0.52 | 0.3 | 2.92 | 0.2 | 0.1 | 0.3 |
| **Standard deviation/Mean** | - | - | - | - | - | - | 0.15 | 0.15 | 0.15 |

**Table 1.** Input parameters for the case for Monte-Carlo simulation study

Two methodologies can be found to estimate the two quantities in Eq. 5. The first one is based on field data, and the second one is based on binder concentration.

## 2.1 Determination of PDF of $q_u$ from field data

Some researchers have been conducted on evaluating the two parameters in Eqs. (5) and (6) (e. g.[21,29-31],). Larsson's (2001) approach[29] involves extraction of soil samples from field deep mixing columns using split-tube-sampler. Larsson's (2001, 2005a, 2005b) work[21,29,30] demonstrates the feasibility of studying the uniformity of binder contents in a cement-admixed column using the statistical analysis. The mean value and variance is given by

$$\begin{cases} \mu_{qu} = \sum_{j=1}^{3} \sum_{i=1}^{n_s} \left(a_{ij} \times \alpha_i\right) \Big/ 3\times\sum_{i=1}^{n_s} \alpha_i \\ \sigma_{qu}^2 = \sum_{j=1}^{3} \sum_{i=1}^{n_s} \left[\left(a_{ij} - \mu_{qu}\right)^2 \times a_i\right] \Big/ (3\times\sum_{i=1}^{n_s} \alpha_i - 1) \end{cases} \quad (6)$$

As shown in **Figure 4**, the samples are numbered from the centre of the column, i = 0 to 5. The samples are drawn in three directions from the centre of the column, numbered j = 1 to 3. The coefficient represents the area ratio which the samples represent.

| $i$ | $\alpha_i = A_i/A_1$ |
|---|---|
| 0 | 1 |
| 1 | 7 |
| 2 | 13 |
| 3 | 20 |
| 4 | 26 |
| 5 | 33 |

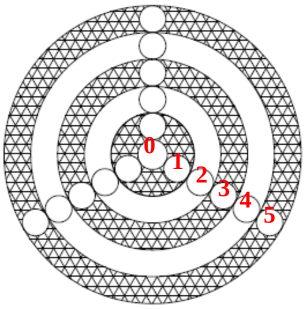


**Figure 4.** Layout of the sample locations and the area ratio (Modified from [31])

## 2.2 Determination of PDF of $q_u$ from mix ratio

As given in Eqs. 2 and 3, the statistical characteristics of $q_u$ can been derived from those of three mass ratios; namely, c, w and s. As discussed earlier, these three mass ratios can be treated as equally variable. Various researchers have examined the variability of the binder concentration, which is directly related to the mass ratio of cement. The binder concentration of DM columns is known to be highly variable (e.g.[17-19, 21-24,32]), but much remains uncertain about the nature of the variation. Since these three mass ratios are not independent as they have the relation of c+w+s=1, two independent state variables can be used sufficiently. Following the form of Eq. 2, the state variables can be selected as s/c and w/c.[31] has conducted centrifuge model tests to capture the variability in s/c and w/c. Table 2 listed a set of s/c and w/c values from centrifuge model tests. Thus, if the statistical characteristics of the mix ratio are controllable, the PDF of $q_u$ is predictable and controllable as well. It is complex task to control the variability in the mix ratio, especially considering the mix quality. In[28], it found that the blade rotation number is a good index to be related to the variation in mass ratio of cement, and the established a predictive formula between the coefficients of variation of mass ratio of cement and the blade rotation number. However, it is not an easy task to reflect the curing effect from centrifuge model tests. In this study, a statistical evaluation model for the time-dependent strength of cement-admixed marine clay is discussed.

| No. | s/c | w/c | No. | s/c | w/c | No. | s/c | w/c |
|---|---|---|---|---|---|---|---|---|
| 1 | 4.25 | 3.15 | 14 | 7.27 | 5.36 | 27 | 4.47 | 3.28 |
| 2 | 4.94 | 3.56 | 15 | 7.09 | 5.25 | 28 | 4.45 | 3.27 |
| 3 | 4.79 | 3.47 | 16 | 4.51 | 3.31 | 29 | 4.61 | 3.37 |
| 4 | 4.37 | 3.22 | 17 | 6.53 | 4.92 | 30 | 5.41 | 3.85 |
| 5 | 7.07 | 5.24 | 18 | 7.33 | 5.4 | 31 | 6.46 | 4.87 |
| 6 | 6.87 | 5.12 | 19 | 6.25 | 4.75 | 32 | 4.45 | 3.27 |
| 7 | 8.59 | 6.16 | 20 | 4.19 | 3.12 | 33 | 6.41 | 4.84 |
| 8 | 4.52 | 3.31 | 21 | 4.16 | 3.09 | 34 | 6.37 | 4.82 |
| 9 | 4.57 | 3.34 | 22 | 6.57 | 4.94 | 35 | 6.69 | 5.01 |
| 10 | 4.65 | 3.39 | 23 | 6.45 | 4.87 | 36 | 6.45 | 4.87 |
| 11 | 4.45 | 3.27 | 24 | 6.78 | 5.07 | 37 | 4.34 | 3.2 |
| 12 | 4.51 | 3.3 | 25 | 6.96 | 5.18 | 38 | 4.45 | 3.27 |
| 13 | 4.36 | 3.22 | 26 | 6.93 | 5.16 | 39 | 4.28 | 3.17 |

**Table 2.** Database of state variables from centrifuge model tests (after [31])

# 3. Time-dependent PDF of $q_u$

One of the advantage of the strength function Eq. 2 over Eq. 1 is that the former takes the curing time effect into account. As a result, the strength is time-dependent, and the PDF of $q_u$ is also time-dependent. Based on the input parameters shown in Table 1, one can plot the PDFs at various curing time. For instance, Figures 5a, 5b and 5c show the PDFs at 7, 28, and 90 days of curing time. It can be found from those figures that, with the increase of curing time, the PDF shifts towards right and also the variation becomes greater. In other words, the mean and variance of the PDF are both varying. This problem can be simplified by considering the form of Eq. 3; that is, considering the term $\ln(q_u)$. For a given curing time, the sources of variation resulted from the mix ratio; whereas, for a fixed mix ratio, the variation resulted from the curing time. In other words, the term $\ln\left\{\left(\frac{q_\infty}{at}\right)^r+1\right\}$ in Eq. 3 is time-dependent, and the terms $m(\frac{s}{c})$, $n\ln(w)$ and $n\ln(c)$ depend on the state variables. Thus, with the increase of curing time, the variance of Eq. 3 will keep unchanged; whereas, the mean value will change as a result of the change in the term $\ln\left\{\left(\frac{q_\infty}{at}\right)^r+1\right\}$. Therefore, when considering the term $\ln(q_u)$, only the mean value is varying. Geometrically speaking, the PDF of $\ln(q_u)$ is purely shift along the strength direction, while the shape keep unchanged. This can be illustrated by **Figure 6**, where the curing time of 7, 28 and 90 days are considered. It can be seen from **Figure 6** that the PDF shape keeps unchanged. Recall that if one consider Eq. 2, both the mean and variance are time-dependent. Thus, by considering Eq. 3, the time-dependent PDF reduces from a second-order problem to a first-order problem. The variance of Eq. 3 is time invariant, which can also be proofed analytically as shown below.

Considering two different curing time but with the same mix ratio with Eq. 2:

$$q_{u1} = q_\infty \left\{1-\frac{1}{1+(\frac{at_1}{q_\infty})^r}\right\}\left\{\frac{\exp\left(m\left(s/c\right)\right)}{\left(\frac{w}{c}\right)^n}\right\} \quad (7)$$

$$q_{u2} = q_\infty \left\{ 1 - \frac{1}{1+(\frac{at_2}{q_\infty})^r} \right\} \left\{ \frac{\exp\left(m\left(s/c\right)\right)}{\left(\frac{w}{c}\right)^n} \right\} \quad (8)$$

The mean and standard deviation of Eqs. 8 and 9 can be written as

$$\mu\left\{q_{u1}\right\} = q_\infty \left\{ 1 - \frac{1}{1+(\frac{at_1}{q_\infty})^r} \right\} E \left\{ \frac{\exp\left(m\left(s/c\right)\right)}{\left(\frac{w}{c}\right)^n} \right\} \quad (9)$$

$$\sigma\left\{q_{u1}\right\} = q_\infty \left\{ 1 - \frac{1}{1+(\frac{at_1}{q_\infty})^r} \right\} S \left\{ \frac{\exp\left(m\left(s/c\right)\right)}{\left(\frac{w}{c}\right)^n} \right\} \quad (10)$$

$$\mu\left\{q_{u2}\right\} = q_\infty \left\{ 1 - \frac{1}{1+(\frac{at_2}{q_\infty})^r} \right\} E \left\{ \frac{\exp\left(m\left(s/c\right)\right)}{\left(\frac{w}{c}\right)^n} \right\} \quad (11)$$

$$\sigma\left\{q_{u2}\right\} = q_\infty \left\{ 1 - \frac{1}{1+(\frac{at_2}{q_\infty})^r} \right\} S \left\{ \frac{\exp\left(m\left(s/c\right)\right)}{\left(\frac{w}{c}\right)^n} \right\} \quad (12)$$

where $\mu$ and $\sigma$ are the expectation and standard deviation operators, respectively. The COV of $q_{u1}$ and $q_{u2}$ can therefore be calculated as:

$$\delta\left\{q_{u1}\right\} = \frac{\sigma\left\{q_{u1}\right\}}{\mu\left\{q_{u1}\right\}} = \sigma \left\{ \frac{\exp\left(m\left(s/c\right)\right)}{\left(\frac{w}{c}\right)^n} \right\} / \mu \left\{ \frac{\exp\left(m\left(s/c\right)\right)}{\left(\frac{w}{c}\right)^n} \right\} \quad (13)$$

$$\delta\left\{q_{u2}\right\} = \frac{\sigma\left\{q_{u2}\right\}}{\mu\left\{q_{u2}\right\}} = \sigma \left\{ \frac{\exp\left(m\left(s/c\right)\right)}{\left(\frac{w}{c}\right)^n} \right\} / \mu \left\{ \frac{\exp\left(m\left(s/c\right)\right)}{\left(\frac{w}{c}\right)^n} \right\} \quad (14)$$

where $\delta$ denotes the COV operator. By comparing Eqs. 10 and 11, one can find that, with the increase of curing time, the COV is invariant. Thus, Eq. 6 is invariant with time, and the shape of the PDF of $\ln(q_u)$ is therefore invariant with time.

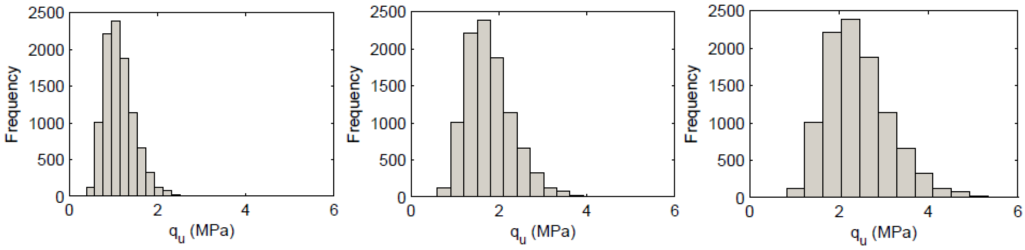


(**a**) (**b**) (**c**)

**Figure 5.** Histograms of unconfined compressive strength at various curing time (**a**) 7 days, (**b**) 28 days and (**c**) 90 days

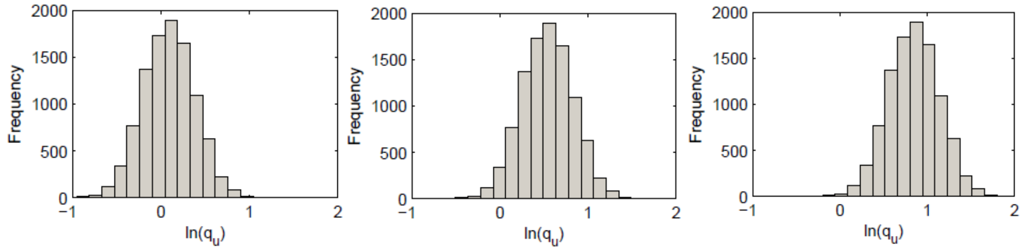


(**a**) (**b**) (**c**)

**Figure 6.** Histograms of natural logarithm of unconfined compressive strength at various curing time (**a**) 7 days, (**b**) 28 days and (**c**) 90 days

# 4. Conclusions

This study introduces the derivation of a statistical framework for strength prediction for DCM treated soft clay. The PFD of the strength of cement improved soft soil may be assumed to follow a lognormal distribution. The probability density function of the strength is a time-dependent variable, so that the curing time effect can be accounted for. In this time-dependent model, only the mean value of the probability density function is varying; as a result, the model is first-order in terms of the varying terms, which is relatively simple compared to other second-order models. The engineering implications of this study lie in the evaluation of the non-uniformity of cement-admixed marine clay. As the mix ratios can be reflected by centrifuge model tests (e.g. [28]) and the curing time effect is considered by [16] and [9], the proposed model is able to predict the strength of the cement improved soil prior to construction. This is likely to benefit the quality control of a deep cement mixing project as well as design for the underground construction such as deep excavation and tunnelling.

# References

1. Liu Y, Quek ST, Lee FH. (2016). Translation random field with marginal beta distribution in modelling material properties. Structural Safety 61: 57-66.
2. Rathmayer H. (1996). Deep mixing methods for soft subsoil improvement in the Nordic countries. Proc. 2nd International Conference on Ground Improvement Geosystems, Tokyo, 2: 869-878.
3. Probaha A. (1998). State of the art in deep mixing technology: Part 1. Basic concepts and overview of technology. Ground Improvement 2(2): 81-92.
4. Bruce DA, Bruce MEC. (2003). The practitioner's guide to deep mixing. Proc. 3rd International Conference on Grounting and Ground Treatment, New York, 120: 474-488.
5. Kamon M. (1996). Effects of grouting and DMM on big construction projects in Japan and the 1995 Hyogoken-Nambu earthquake. Proc. 2nd International Conference on Ground Improvement Geosystems, Tokyo, (2): 807-823.
6. Bahador M, Pak A. (2012). Small-strain shear modulus of cement-admixed kaolinite. Geotechnical and Geological Engineering 30: 163–171.
7. Flores RD, Di Emidio G, Van Impe WF. (2010). Small-strain shear modulus and strength increase of Cement-Treated clay. Geotechnical Testing Journal, 33(1): 62-71, https://doi.org/10.1520/GTJ102354.
8. Xiao H. (2017). Evaluating the stiffness of chemically stabilized marine clay. Marine Georesources & Geotechnology 35(5): 698-709.
9. Xiao H, Shen W, Lee FH. (2017a). Engineering properties of marine clay admixed with Portland cement and blended cement with siliceous fly ash. Journal of Materials in Civil Engineering, ASCE, 29(10): 04017177.
10. Xiao H, Wang W, Goh SH. (2017b). Effectiveness study for fly ash cement improved marine clay. Construction

and Building Materials, 157: 1053–1064.
11. Xiao H, Lee FH, Yao K, Ho J, Liu Y. (2018a). Miniature LVDT setup for local strain measurement on cement-treated clay specimens. Marine Georesources & Geotechnology.
12. Xiao H, Yao K, Liu Y, Goh SH, Lee FH (2018b). Small strain shear modulus study with bender element testing for cement-treated marine clay. Construction and Building Materials, 172: 433-447.
13. Gallavresi F. (1992). Grouting improvement of foundation soils. Proc. Grouting, Soil Improvement and Geosynthetics, ASCE, New York, 30: 1-38.
14. Nishida K, Koga Y, Miura N. (1996). Energy consideration of the dry jet mixing method. Proc. 2nd International Conference on Ground Improvement Geosystems, Tokyo, (1): 643-748.
15. Lee FH, Lee Y, Chew SH. (2005). Strength and modulus of marine clay-cement mixes. Journal of Geotechnical and Geoenvironmental Engineering 131(2): 178-186.
16. Xiao HW, Lee FH, Chin KG. (2014). Yielding of cement-treated marine clay. Soils and Foundations, 54(3): 488-501.
17. Honjo Y. (1982). A probabilistic approach to evaluate shear strength of heterogeneous stabilized ground by deep mixing method. Soils and Foundations 22(1): 23-38.
18. Babasaki R, Terashi M, Suzuki T, Maekawa A, Kawamura M, Fukazawa E. (1997). JGS TC Report: Factor influencing the strength of the improved soil. Proc. Grouting and Deep Mixing, The 2nd International Conference on Ground Improvement Geosystems, A.A. Balkema, 913-918.
19. CDIT (Coastal Development Institute of Technology), J. (2002). The deep mixing method: principle, design, and construction, Swets & Zeitlinger Publishers, Lisse ; Exton, PA.
20. Larsson S. (2003). Mixing processes for ground improvement by deep mixing. Ph.D, Royal Institute of Technology, Stockholm, Sweden, Stockholm.
21. Larsson S, Dahlstrom M, Nilsson BA. (2005). Uniformity of lime-cement columns for deep mixing: a field study. Ground Improvement 9(1): 1-15.
22. Lee FH, Lee CH, Dasari GR. (2006). Centrifuge modeling of wet deep mixing processes in soft clays. Géotechnique, 56(10): 677-691.
23. Lee FH, Lee CH, Dasari GR. (2008). Centrifuge study on uniformity of wet deep mixing. International Journal of Physical Modelling in Geotechnics 8(1): 1-20.
24. Chen J, Lee FH, Ng CC. (2011). Statistical analysis for strength variation of deep mixing columns in Singapore. GeoFrontiers 2011: Advances in Geotechnical Engineering (GSP 211), Han J, Alzamora DE, eds., Geo-Institute, ASCE, Dallas, TX, 576-584.
25. Probaha A. (2002). State of the art in quality assessment of deep mixing technology. Ground Improvement, 6(3): 95-120.
26. Liu Y, Zheng JJ, Guo J. (2008). Statistical evaluation for strength of pile by deep mixing method. In Geotechnical Engineering for Disaster Mitigation and Rehabilitation (Editors Liu H.L *et al*.) Springer, Berlin, Heidelberg.
27. Liu Y, Lee FH, Quek ST, Chen EJ, Yi JT. (2015). Effect of spatial variation of strength and modulus on the lateral compression response of cement-admixed clay slab. Géotechnique. 65(10): 851-865.
28. Chen EJ, Liu Y, Lee FH. (2016). A statistical model for the unconfined compressive strength of deep-mixed columns. Géotechnique 66(5): 351-365.
29. Larsson S. (2001). Binder distribution in lime-cement columns. Ground Improvement, 5(3): 110-122.
30. Larsson S, Dahlstrom M, Nilsson BA. (2005b). A complementary field study on the uniformity of lime-cement columns for deep mixing. Ground Improvement 9(2): 67-77.
31. Chen J. (2012). Centrifuge model study of mixing quality in wet deep mixing. Doctor of Philosophy, National University of Singapore, Singapore.
32. Lee FH, Chin KG, Xiao H, Chen J. (2013). Cement-soil treatment in underground construction. Indian Geotechnical Conference 2013, Roorkee, India.